International Journal of Biological Macromolecules xxx (xxxx) xxx

Contents lists available at ScienceDirect

International Journal of Biological Macromolecules

journal homepage: http://www.elsevier.com/locate/ijbiomac

Paper-based biosensor based on phenylalnine ammonia lyase hybrid nanoflowers for urinary phenylalanine measurement

Baoting Sun, Zichen Wang, Xiaoyi Wang, Mengxia Qiu, Zhijin Zhang, Ziyuan Wang, Jiandong Cui *, Shiru Jia *

State Key Laboratory of Food Nutrition and Safety, Key Laboratory of Industrial Fermentation Microbiology, Ministry of Education, Tianjin University of Science and Technology, No 29, 13th, Avenue, Tianjin Economic and Technological Development Area (TEDA), Tianjin 300457, PR China

ARTICLE INFO

Article history:
Received 30 August 2020
Received in revised form 26 October 2020
Accepted 27 October 2020
Available online xxxx

Keywords:
Enzyme immobilization
Hybrid nanoflowers
Phenylalnine ammonia lyase
PKU detection
Biosensor

ABSTRACT

The Phenylketonuria (PKU) is an inborn defect of phenylalanine (Phe) metabolism, in which Phe accumulated in the blood causing alterations at the central nervous system. Therefore, the detection of PKU is very important for the early diagnosis of PKU patients. However, existing tests for PKU are time-consuming and require high-resource laboratories. In this study, a novel paper-based biosensor based on phenylalnine ammonia lyase (PAL) hybrid nanoflowers was constructed that provides a semi-quantitative output of the concentration of Phe from urine samples. PAL@$Ca_3(PO_4)_2$ hybrid nanoflowers (PAL@NF) were first prepared using PAL and Ca^{2+}. Synthesis conditions of the PAL@NF on the formation of the PAL@NF were optimized. The PAL@NF exhibited 90% activity recovery under optimal condition. Compared with free PAL, the PAL@NF displayed good storage stability and increased tolerance to proteolysis. After five consecutive operating cycles, the PAL@NF still retained 73% of its initial activity, indicating excellent reusability. Furthermore, the paper-based biosensor was able to detect Phe concentration in urine samples, and exhibited good linearity to the Phe concentrations in the range from 60 to 2400 μM and the response time was only about 10 min. Therefore, the paper-based biosensor can be a promising candidate as a biosensor for the detection of PKU.

1. Introduction

Phenylketonuria (PKU) is an inborn defect in essential amino acid phenylalanine (Phe) metabolism that causes the failure of Phe to be converted into tyrosine due to the deficient phenylalanine hydroxylase (PAH) [1]. Therefore, a large number of Phe is accumulated in the body and causes serious brain injury and neurocognitive dysfunction in patients [2]. The diagnosis of PKU is of importance to prevent these clinical anomalies. Nowadays, the diagnosis methods of PKU patient include newborn screening procedures, guthrie bacterial suppression test in the first days of life [3], high performance liquid chromatography [4,5], and tandem mass spectrometry analysis [6]. However, these detection methods are high cost for periodic inspections and the sample pretreatment processes are tedious. Furthermore, it will take several days to analyze the test results, thus delaying the treatment time for many PKU patients. Consequently, it is ideal to develop an instrument-free, fast, easy and low-cost test for PKU patients to monitor their Phe levels. Phenylalnine ammonia lyase (PAL, EC 4.3.1.24) is the rate-limiting enzyme in phenylpropane metabolism in plants. It can catalyze L-Phe to produce trans cinnamic acid (t-CA) and NH_3. In recent years, PAL has been considered as as a potential substitution therapy for PKU [2,7–9]. For example, PAL modified with polyethylene glycol has been used for detection and treatment of PKU [9]. However, the activity of modified PAL exhibited a great loss compared with that before modification. Furthermore, the extraction and purification process led to the loss of PAL activity [10]. Therefore, complexity of extraction process, the low availability, and poor stability have been limited application for detection and treatment of PKU with PAL.

Recently, a new enzyme immobilization method, called enzyme-inorganic hybrid nanoflowers (HNFs) technology was developed by Ge et al. [11]. HNFs have been widely used in biological sensing and biocatalysis due to their excellent catalytic performance and simple preparation process. The formation process of HNFs includes three steps: nucleation, growth, and completion [11–13]. Generally, the traditional immobilization methods can result in the obstruction of mass transfer between enzymes and substrates, the coverage of active sites, and conformation changes of enzymes, thus causing the low immobilization efficiency and activity [14–18]. Compared with the traditional immobilization enzyme, the HNFs have high specific surface area and low mass transfer restriction due to the multi-layered flower-like structure, thus exhibiting enhanced catalytic activity. In the past ten years, HNFs containing various enzymes have been prepared, such as laccase-HNFs [19], horseradish peroxidase (HRP)-HNFs [20,21], lactoperoxidase-HNFs [22], glucose oxidase (GOx)-HNFs [23], lipase-HNFs [24,25], and α-amylase-HNFs [26]. In addition to enzyme

* Corresponding authors.
E-mail addresses: cjd007cn@163.com (J. Cui), jiashiru@tust.edu.cn (S. Jia).

https://doi.org/10.1016/j.ijbiomac.2020.10.218
0141-8130/

molecules, some biomolecules such as DNA [13,27–29], caffeine [30], IgG [31], Cytochrome P450 [32], other biomolecules [33–37] and orgnaic molecules [38,39] have been immobilized as HNFs. Recent years, variety of biosensors based on HNFs have been synthesized for disease diagnostics, detection and bioanalytical applications [40,41]. For example, HRP/GOx@$Cu_3(PO_4)_2$ HNFs have been used as a fast and accurate biosensor for detection of live pathogenic bacteria in urine. The HNF biosensor exhibited a low detection limit of 1 CFU mL^{-1}, and the response time was only about 140 min [42]. Laccase-$Cu_3(PO_4)_2$ HNFs on cellulose acetate membrane was applied as a rapid and on-site biosensor for detection of phenol, and displayed different visible colors and a linear relationship between phenol concentration of 0.4–50 μg/mL [43]. In addition, GO_x-copper hybrid nanoflowers with Fe_3O_4 magnetic nanoparticles exhibited superior peroxidase-mimicking activity as well as substrate channeling for glucose detection [44]. Furthermore, the same group developed a mediatorless glucose biofuel cell based on hybrid nanoflowers incorporating GO_x and catalase [45].

Recently, the paper-based biosenors has attracted much interest because of their low cost, the preparation of simple, and easy to operate. For example, the paper-based biosensors were developed for detection of Phe in blood [46,47], In addition, a paper-based biosenor coupled to electrochemical detection was constrcuted using PAH. The paper-based biosenor could detect efficiently the concentration of Phe in blood [48,49]. However, the blood test is invasive, and draw blood for infants is difficult. Compared with the blood test, a urine test is noninvasive and likely to lead to higher patient compliance.

The purpose of this study was the development of a novel paper-based biosensor based on PAL hybrid nanoflowers for urinary Phe measurement. For the construction of the paper-based biosensor, PAL-$Ca_3(PO_4)_2$ hybrid nanoflowers (PAL@NF) were firstly prepared using crude PAL from recombinant BL21(DE3) *E. coli*. The catalytic performance of the PAL@NF were investigated. Then, the PAL@NF was adsorbed on the surface of filter paper to obtain the paper-based biosensor. PAL in the paper-based biosensor can catalyze Phe in urine to produce a quantitative amount of t-CA which can be oxidized by the addition of a small amount of potassium permanganate, causing the fade of potassium permanganate. This color variation is well appreciate by human eyes. As a result, users will be able to determine the concentration of Phe in a urine sample by colorimetric comparison with a chromatic scale.

2. Materials and methods

2.1. Materials

Yeast extract and tryptone were purchased from Thermo Fisher Scientific (Shanghai, China). Typsin (250.N.F·U/mg), Isopropyl-β-D-Thiogalactoside (IPTG) and trimethylolamine were obtained from Beijing Solarbio Science & Technology Co., Ltd. (Beijing, China). L-Phe was purchased from Aladdin Reagent Co., Ltd. (Shanghai, China). Filter papers were purchased from Whatman (Shanghai, China). Phosphates, $CaCl_2$, NaCl, ammonium sulfate, potassium permanganate and other reagents were purchased from Fuchen Chemical Reagent Co., Ltd. (Tianjin, China). The PAL recombinant BL21 (DE3) *E. coli* cells were stored in our lab.

2.2. Production and crude extraction of PAL

PAL recombinant BL21 *E. coli* was incubated in LB medium containing 30 μg/mL kanamycin at 37 °C. After 16 h, 0.1 mM IPTG was added to induce PAL expression at 20 °C. After 12 h, culture medium was centrifuged at 8000 rpm for 10 min at 4 °C, and cells were washed three times with cold deionized water, and sonicated until the solution became clear. After centrifugation, PAL in the supernatant was precipitated by 40% ammonium sulfate. After centrifugation, precipitates were dissolved by 50 mM Tris-HCl buffering (pH 8.0), recombinant PAL proteins in the solution was purified by a 5 mL nickel Sepharose 6 Fast Flow column, the purified PAL proteins were collected and analyzed by SDS-PAGE.

2.3. Preparation of PAL@NF

For the PAL@NF, a certain amount of $CaCl_2$ solution was added into PBS (pH 7.4, 200 mM) containing PAL, and the mixture solution was incubated for 12 h at 4 °C. After centrifugation, the obtained PAL@NF was washed three times with MiliQ water. Besides, effects of PAL concentration (0.1 mg/mL–2.0 mg/mL), Ca^{2+} concentration (6 mM–18 mM), and phosphate concentration (5 mM–50 mM) on the formation of the PAL@NF.

2.4. PAL activity assay

The PAL activity was determined by the previous reports [11]. Briefly, PAL samples were mixed with 50 mM Tris-HCl buffer (pH 8.8) and 25 mM L-Phe at 40 °C. After 10 min, 1 M of HCl was added to terminate the reaction. After centrifugation, A_{278} of the supernatant was tested with a spectrophotometer. 1 U PAL activity was defifined as the amount of PAL required to produce 1 μmol of t-CA per min.

The PAL activity recovery in the PAL@NF was calculated as given in Eq. 1.

$$\text{Activity recovery}(\%) = \frac{\text{Total activity of PAL@NF(U)}}{\text{Total free activity of PAL(U)}} \times 100 \quad (1)$$

2.5. PAL@NF stability

Storage stability of free PAL and PAL@NF under room temperature was tested for 20 days and the residual activities of PAL were tested every 2 days. The pH stability of the free and PAL@NF was measured in the pH range of 7–11. Besides, to test the resistance to proteolysis, free PAL and PAL@NF were incubated in 50 mM Tris-HCl buffer (pH 8.8) containing 1 mg/mL of trypsin for 2–10 min at 40 °C, respectively. Reusability of the PAL@NF was examined by means of ten repetitive measurements using 25 mM L-Phe.

2.6. The kinetic parameters

The K_m and V_{max} were obtianed by determining the initial reaction rates with L-Phe. The concentrations of L-Phe were ranged from 2.5 mM to 50 mM. The K_m value and V_{max} were calculated according to the Michaelis-Menten Eq. (2).

$$V = V\max \times \frac{[s]}{\mathrm{km} + [s]} \quad (2)$$

2.7. Labeling PAL with FITC

1 g of PAL was added into 50 mg/mL FITC solution (dissolved in DMSO) for 1 h without light. Modified FITC labeled PAL were used to prepare PAL@NF.

2.8. Preparation of paper-based biosenor and Phe determination

For preparation of paper-based biosenor, the PAL@NF was immobilized on Whatman # 1 filter paper microzones surface with a diameter of 6 mm by physical adsorption, and dried it at room temperature. For Phe determination, urine samples were added into the paper-based biosenor and incubated for 10 min at 40 °C. Subsequently,

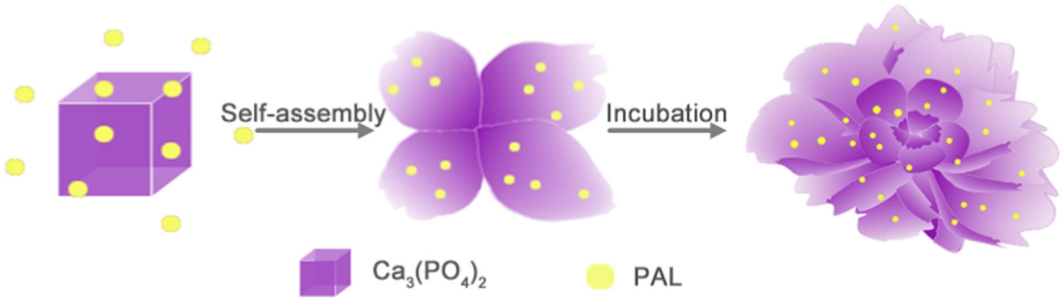

Fig. 1. The synthesis of the PAL@NF.

5 μL potassium permanganate solution (112 mM) was added into the paper-based biosenor.

PAL@NF in the paper-based biosenor catalyzes Phe from the urine samples to t-CA, and the resultant t-CA is oxidized by the addition of potassium permanganate, causing the fade of potassium permanganate. For comparation, a chromatic-scale was established by using simulated urine containing different concentrations of L-Phe (60 μM- 2400 μM).

3. Results and discussion

3.1. Preparation and characterization of PAL@NF

The schematic diagram for the preparation of the PAL@NF was shown in Fig. 1. In the synthesis strategy, the formation of the PAL@NF self-assembly contains three steps: first, primary crystals of $Ca_3(PO_4)_2$ are formed. Second, PAL molecules attach to $Ca_3(PO_4)_2$ crystals by coordination binding between the protein and Ca^{2+}. Finally, nanisotropic growth leads to the formation of nanoflower. SEM images of the prepared PAL@NF in different PAL concentrations was shown in Fig. 2. It was found that flower-like structure appeared when PAL concentration was 0.1–1.0 mg/mL (Fig. 2a-2d). However, with further increase of PAL concentration, the PAL@NF exhibited large amorphous cluster (Fig. 2e and f). The results were consistent with previous reports [50]. These results indicated that the concentration of PAL had significant impact on the formation of PAL@NF. The influences of Ca^{2+} concentration on the morphology of the PAL@NF was shown in Fig. 3. Spherical PAL based hybrid nanostructures were observed when Ca^{2+} concentration was 6 mM (Fig. 3a). With increase of Ca^{2+} concentration, the formation of flower shape PAL@NF were obtained (Fig. 3b, c). However, when Ca^{2+} concentration was increased to 18 mM, PAL@NF with randomly-arranged petal and crystalline structures was obtained (Fig. 3d). The previous reports proved that Ca^{2+} ion is a critical factor to form primary nanocrystals of hybrid nanoflowers [24]. Our results were consistent with previous reports. In addition, influences of phosphate concentration on the formation of the PAL@NF were studied. The results suggested that PAL @NF with flower-like structure appeared when phosphate concentration was at 10 mM (Fig. 3f). However, the other three phosphate concentrations (5 mM, 25 mM and 50 mM) used in

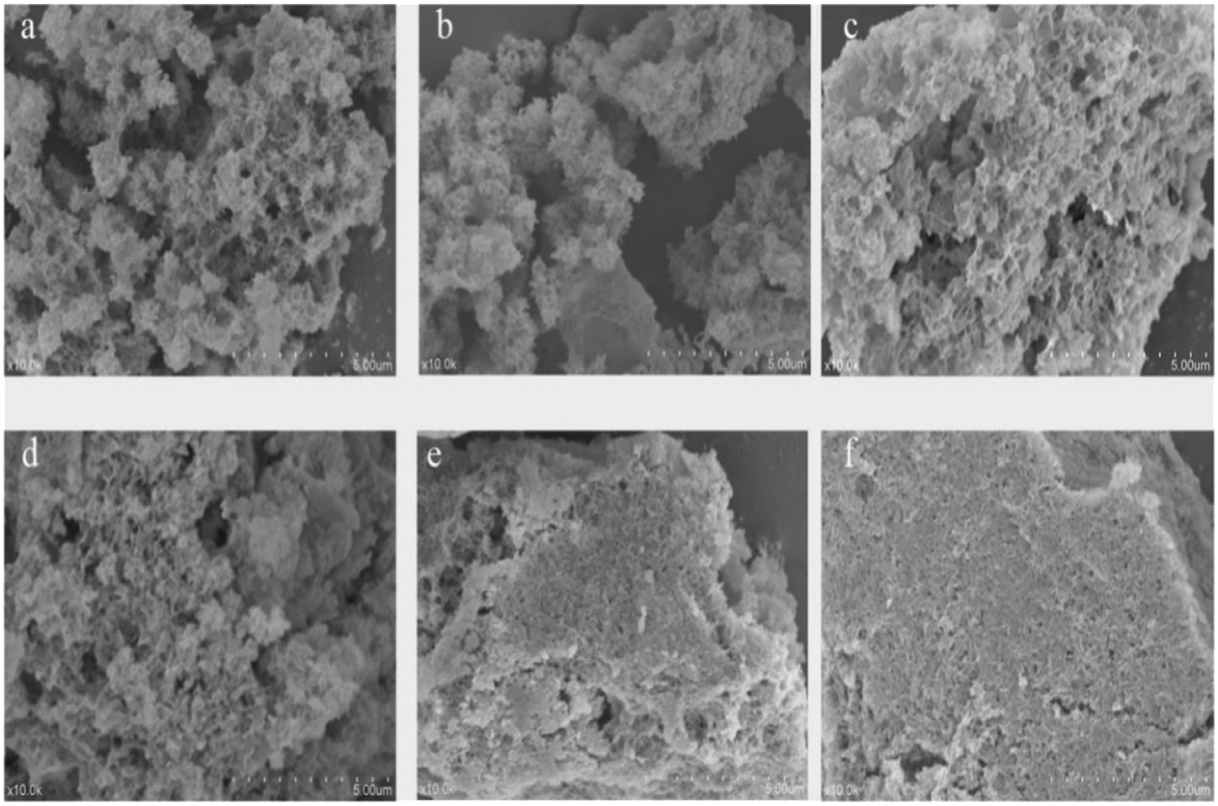

Fig. 2. SEM images of the PAL@NF in different PAL concentrations ((a to f): 0.1 mg/mL(a); 0.25 mg/mL(b); 0.5 mg/mL(c); 1.0 mg/mL(d); 1.5 mg/mL(e); 2.0 mg/mL(f).

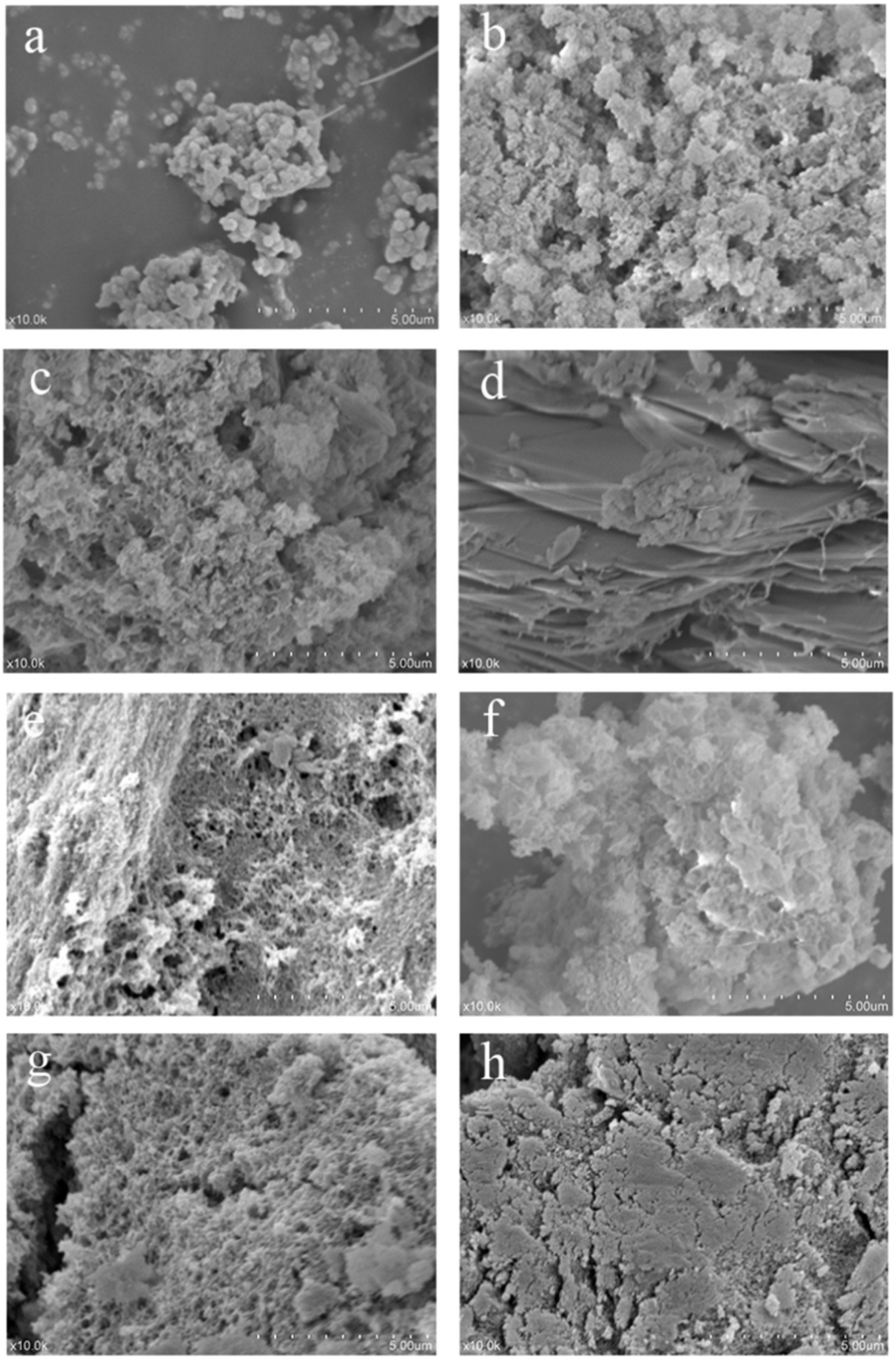

Fig. 3. SEM images of the PAL@NF in different $CaCl_2$ concentrations: 6 mM (a); 12 mM(b); 15 mM (c); 18 mM (d). SEM images of the PAL@NF in different phosphate concentrations: 5 mM (e); 10 mM(f); 25 mM (g); 50 mM (h).

PAL@NF formation did not caused flower-like structure (Fig. 3e, g, h). Besides, it was found that temperature (at 4 °C and room temperature) and pH (at 7.0–10.0) had no significant effect on the formation of the PAL@NF (data not shown). The flower-like shape of the PAL@NF was further demonstrated by TEM images (Fig. 4a). Besides, strong green fluorescence was observed in the CLSM image of the PAL@NF(PAL proteins were labeled by FITC), indicating the presence of PAL in the PAL@NF(Fig. 4b). The FTIR spectra of the PAL@NF, PAL, and $Ca_3(PO)_4$ were

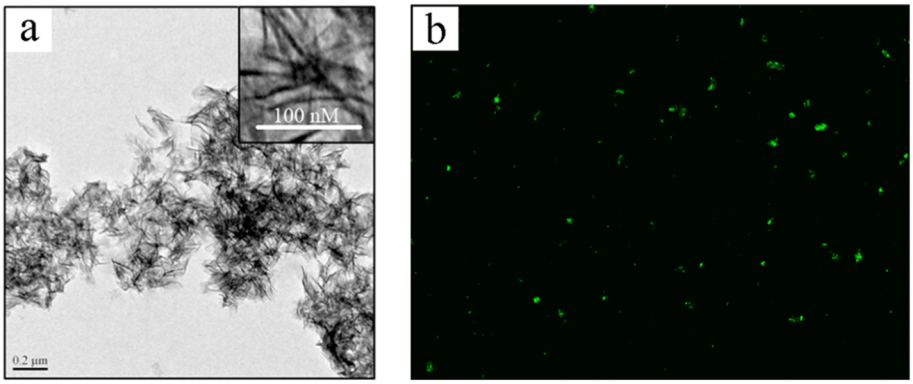

Fig. 4. TEM images of the PAL@NF (a); Fluorescence confocal microscopy images of FITC-PAL@NF (b).

presented in Fig. 5a. The characteristic peaks from 1060 cm^{-1} to 1030 cm^{-1} and from 610 cm^{-1} to 530 cm^{-1} were attributed to the phosphate groups (Fig. 5b and Fig. 5c) [31]. Two strong typical characteristic peaks were observed from 1660 cm^{-1} to 1650 cm^{-1} and from 1580 cm^{-1} to 1500 cm^{-1}, which were ascribed to the amide I and II bands of protein(Fig. 5a and Fig. 5b). Besides, DES results (Fig. 6a and Fig. 6b) clearly indicated the presence of Ca, P, and O in the texture of both the PAL@NF and $Ca_3(PO)_4$. However, C and N were only observed in the PAL@NF, indicating the presence of PAL in the PAL@NF. Therefore, these results demonstrated that the PAL@NF was the successfully prepared.

3.2. Activity of PAL@NF

The previous reports demonstrated that the HNFs had much high catalytic activities because of high protein loading, low diffusion resistance, and mild preparation conditions [51]. Similar to previous reports, the PAL@NF displayed a significantly high activity recovery of 90% (data not shown). Besides, the optimum temperature of both free PAL and the PAL@NF was at 40 °C (Fig. 7a). At the same time, the optimum pH for free PAL and the PAL@NF was at pH 9 (Fig. 7b). These results showed that immobilization procedure did not introduce structural changes of PAL. However, compared with free PAL, the PAL@NF had high K_m value, indicating a lower affinity to substrate. Furthermore, the PAL@NF displayed lower V_{max}/K_m than the free PAL (Table 1). These results indicated that the mass-transfer limitation of the PAL@NF was higher than free PAL.

3.3. Stability of PAL@NF

Reusability is one of the most important parameters of the catalytic performance of immobilization enzymes. Thus, reusability of the PAL@NF was investigated. As shown in Fig. 8, after five consecutive operating cycles, the residual activity of the PAL@NF was still maintained 73% of its original activity (Fig. 8a), indicating good durability. Furthermore, free PAL lost its activity after 8 days under room temperature, whereas the PAL@NF still kept 60% of its initial activity after 19 days. Obviously, the PAL@NF had better storage stability than free PAL (Fig. 8b). The excellent durability and storage stability of the PAL@NF are the key to the robustness of the paper-based biosensor.

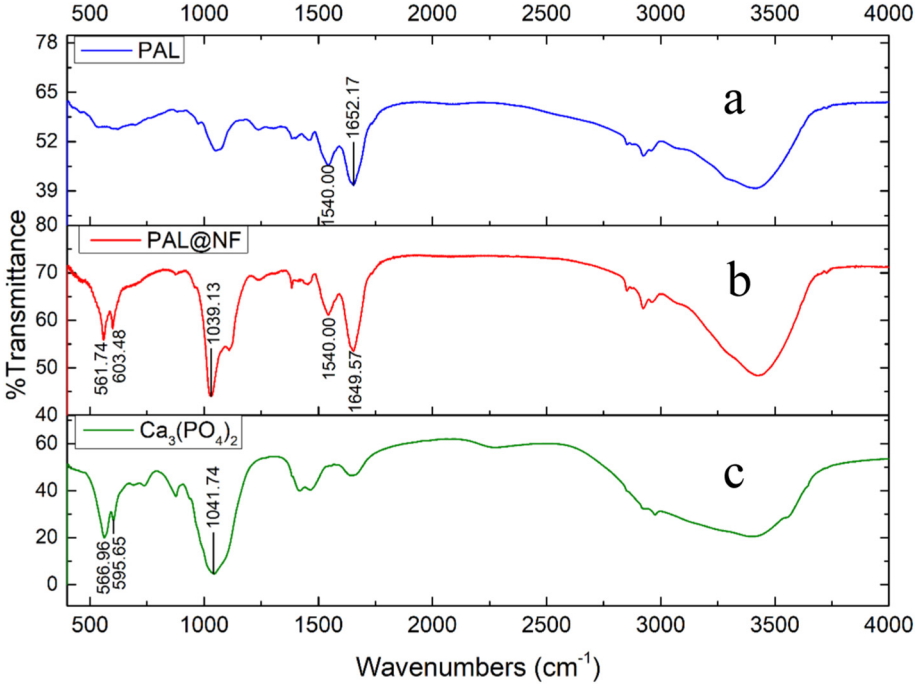

Fig. 5. FT-IR spectra analysis of PAL (a), PAL@NF (b) and $Ca_3(PO_4)_2$ (c).

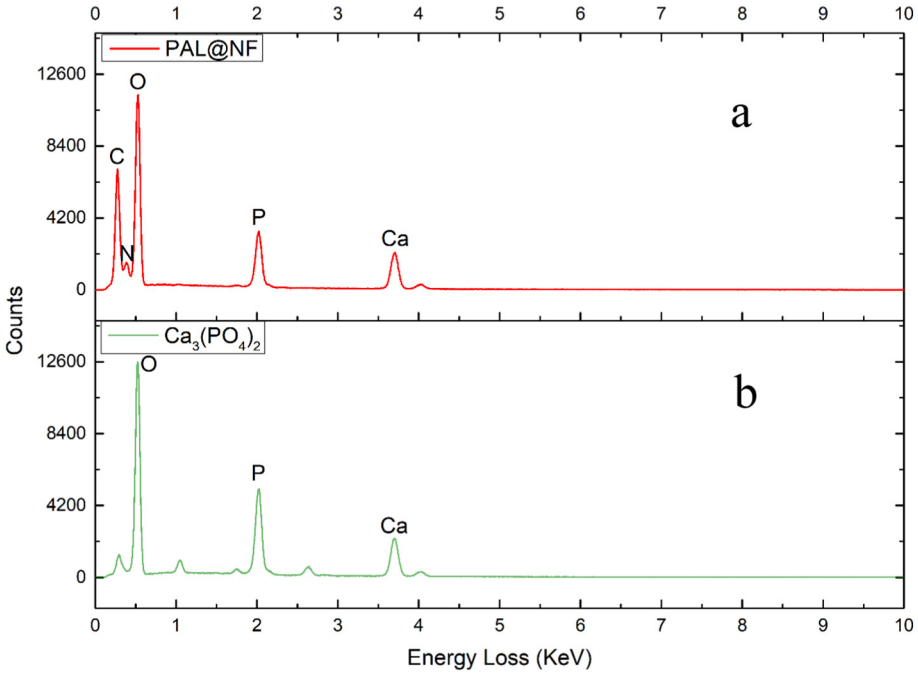

Fig. 6. EDS spectrum of element distribution.

Besides, the pH stability of PAL@NF was also explored. The PAL@NF was more stable than the free PAL in the pH range of 7–11 (Fig. 8c). However, both free PAL and PAL@NF lost activity in acidic environment (pH 3–6). The results indicated that both free PAL and PAL@NF were unstable under acidic conditions. The previous reports proved that PAL enzyme can be easily destroyed by acid [52,53]. For PAL@NF, the structure of nanoflowers was destroyed under acidic conditions, and PAL was released from the PAL@NF, thus causing inactivation. Besides, the PAL@NF exhibited higher tolerance towards trypsin than free PAL (Fig. 8d). Overall, these excellent properties of PAL@NF are very useful for the preparation of paper-based biosensors.

Table 1
Comparison of apparent kinetic parameters of free PAL and PAL@NF.

Enzyme	k_m(mM)	V_{max}(mM/L·min)	V_{max}/K_m
PAL	8.400	0.0273	0.00325
PAL@NF	13.216	0.0205	0.00155

3.4. Detection of Phe in urine samples

The proposed paper-based biosenor based on the following principles: PAL in the PAL@NF catalyzes Phe in urine samples to produce a certain number of t-CA, and the resultant t-CA is oxidized by the addition of potassium permanganate that induces color change in the sample solution. This color change of the sample is easily observed by human eyes. As a result, Phe concentration in the sample can be determined via colorimetric comparison with a chromatic scale. Furthermore, urine samples are easier to obtain than blood samples. In this study, effects of concentrations of urine components (uric acid and urea), urinary pH value (4.0–8.0), and test time on detection of Phe concentration in urine samples were firstly investigated. The results showed that there is no obvious change in color under different concentrations of uric

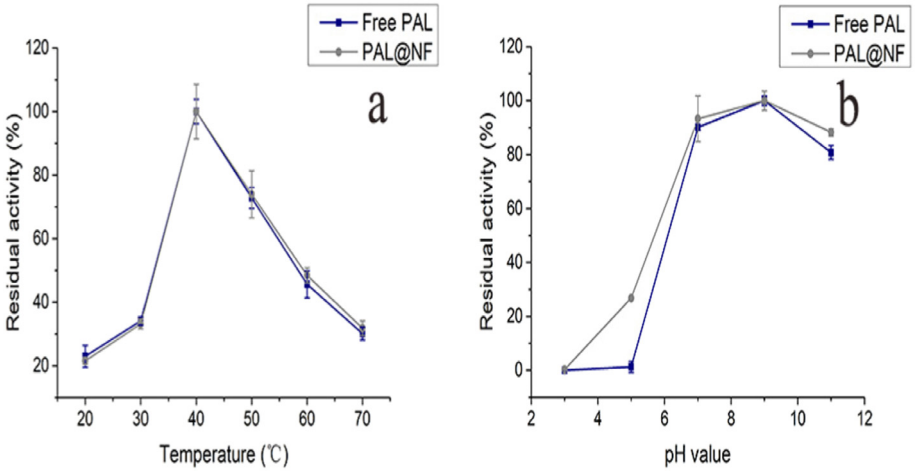

Fig. 7. Optimum temperature and pH of the PAL@NF.

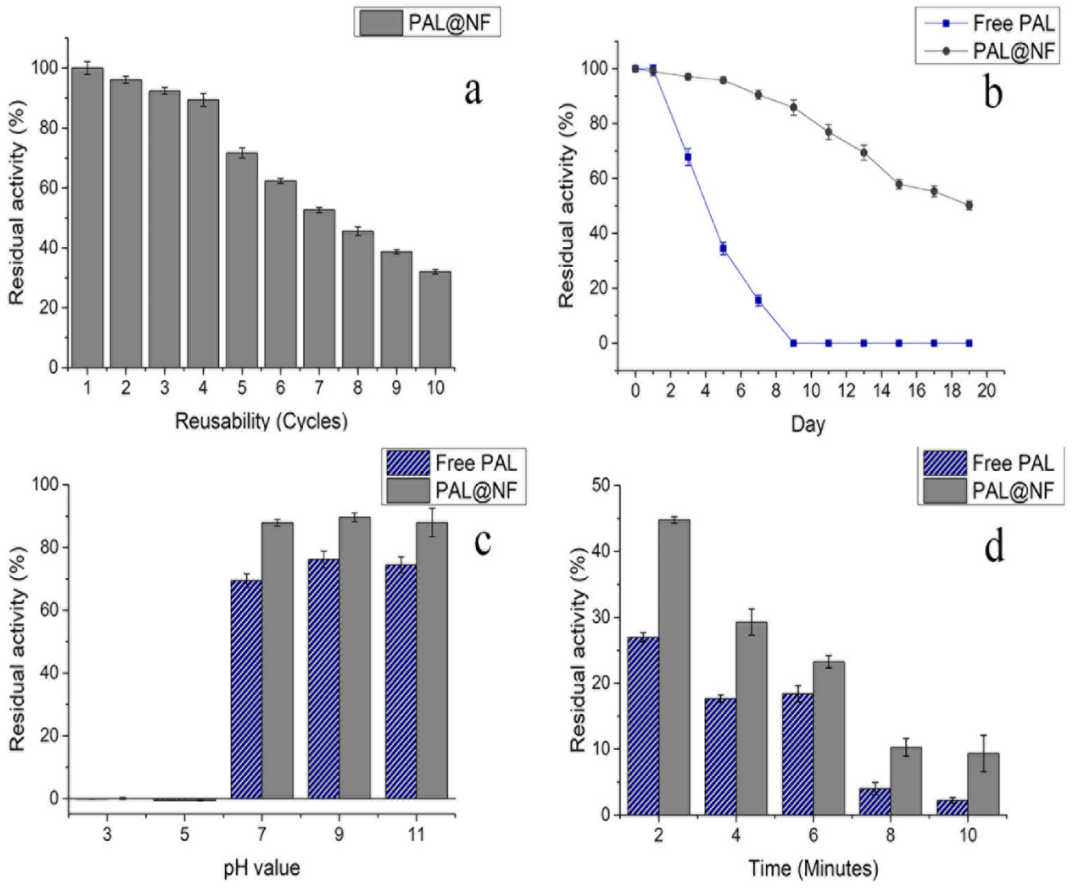

Fig. 8. Reusability of PAL@NF (a); storage stability of the PAL@NF (b); pH stability of PAL@NF (c); the resistance of the PAL@NF to proteolysis (d).

acid (0–300 uM) and urea (0.02–0.1%), indicating that uric acid and urea had no significant effect on the detection of Phe (data not shown). However, urinary pH value (4.0–8.0) and test time exhibited significant effects on the detection for Phe concentration in urine samples. There were no significant color changes for the paper-based biosensors when urinary pH value is at 4.0 and 5.0 (Fig. 9). The results can be explained by the fact that PAL@NF is unstable and inactivated under acidic conditions (Fig. 8c). By contrast, the color change or fading was clearly observed when urinary pH value was at 6.0–8.0 (Fig. 9). The results also showed that the paper-based biosensors could be used to detect Phe concentration in urine samples because of the pH of human urine is usually about 6.0. Besides, test time had significant effects on color changes for the paper-based biosensors. The obvious color change or fading of urine samples containing different Phe concentrations was observed before 5 min. However, no color change or fading was observed after 10 min (Fig. 10). Therefore, the response time of the paper-based biosensors was only about 10 min.

To measure Phe concentration in the urine samples, a chromatic-scale was first constructed by using Phe standard solutions with concentration of 60 to 2400 μM. This color-scale was shown in Fig. 11a. It was found that Phe with concentration of 60–2400 uM has a good correlation compared with the color-scale (Fig. 11b). At the same time, Phe concentration in urine was further proved by HPLC. The standard curve of L-Phe concentration detected by HPLC was shown in Fig. 11c. These results indicated that the detection limit of the paper-based biosensor was estimated at 60 uM, and the dynamic ranging was from 60 μM to 2400 μM. Generally, the urinary Phe value in PKU patients is kept below the 3000 μM [54]. Therefore, the paper-based biosensor for Phe detection on urine sample is a simple, fast, low-cost, and suitable for home applications.

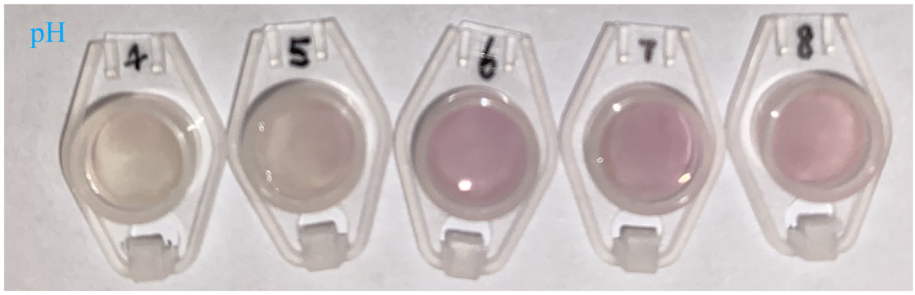

Fig. 9. Effects of urinary pH value (4.0–8.0) on the detection of Phe concentration in urine samples.

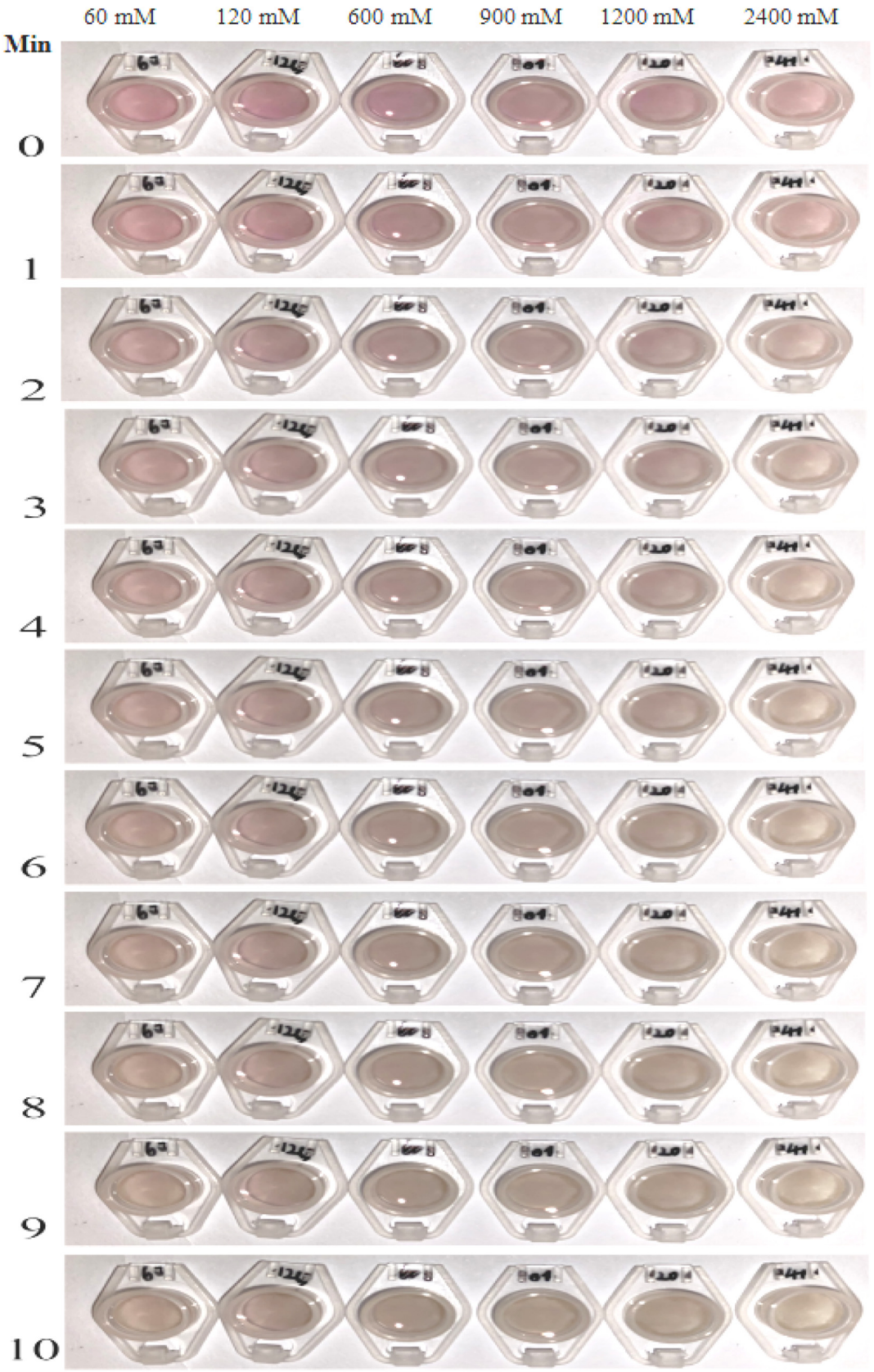

Fig. 10. Effects of test time on the detection of Phe concentration in urine samples.

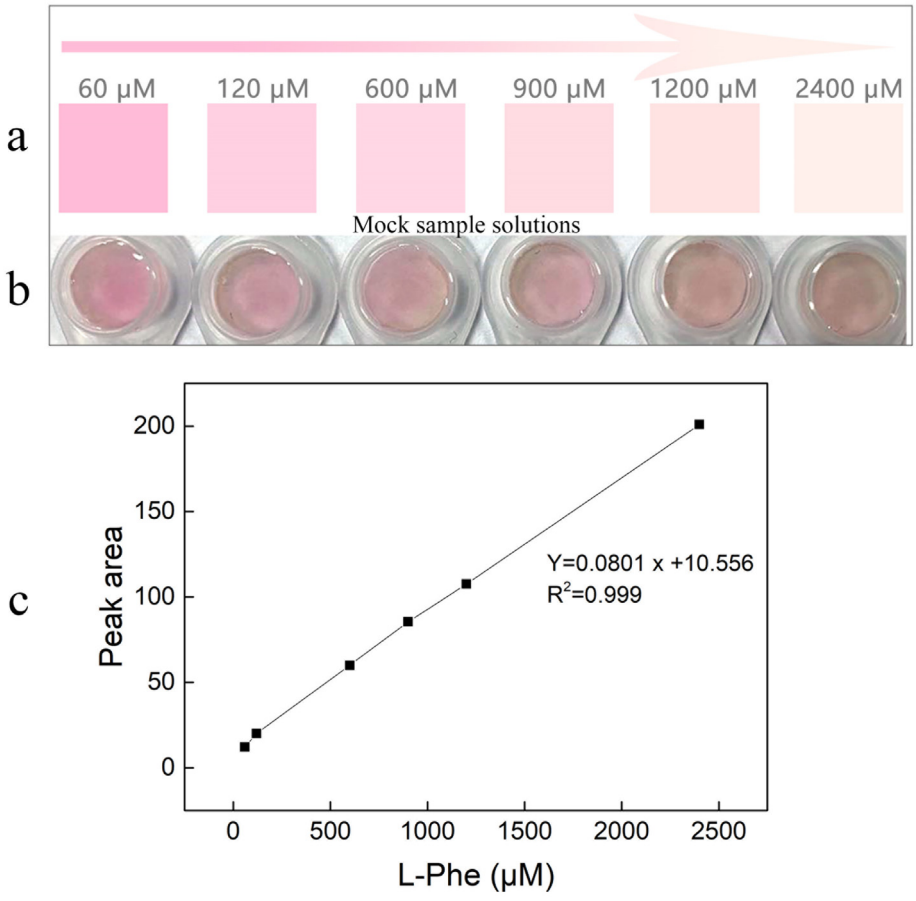

Fig. 11. Correlation of chromatic-scale and intensity with Phe concentration, chromatic-scale (a), The standard curve of Phe concentration detected by HPLC (b).

4. Conclusions

In summary, PAL@NF was successfully prepared by using PAL and $Ca_3(PO_4)_2$. The resultant PAL@NF displayed high activity and stability. Furthermore, a paper-based biosensor based on the PAL@NF for urinary Phe measurement was constructed for the first time. The dynamic range of the paper-based biosensor is 60 μM–2400 μM, and limit of detection is 60 μM. Furthermore, the test time was only about 10 min. Therefore, the paper-based biosensor is expected to become a home-test monitoring for PKU.

Authors statement

Explanation of the manuscript's significance

Phenylketonuria (PKU) is an autosomal recessive inheritance disease and it is one of the most common genetic metabolic disease. The metabolism of essential amino acid phenylalanine (L-Phe) for PKU patients is blocked due to the deficient phenylalanine hydroxylase (PAH), which which leads to the failure of phenylalanine to be converted into tyrosine. Therefore, a large number of L-phe is accumulated in the body and causes serious brain injury and neurocognitive dysfunction in patients. The detection of PKU is very important for the early diagnosis of PKU patients. However, the current methods are either imprecise or time-consuming.

Phenylalnine ammonia lyase (PAL, EC 4.3.1.24) can catalyze L-Phe to produce trans cinnamic acid (t-CA) and ammonia. In recent years, it was found that the PAL can be used for detection and treatment of PKU. However, complexity of extraction process, the low availability, and poor stability have been limited application for detection and treatment of PKU with PAL. Enzyme-inorganic hybrid nanoflowers (HNFs) are an efficient immobilization method. Recent years, variety of biosensors based on HNFs have been synthesized for disease diagnostics and detection due to their better biocompatibility, enhanced catalytic activity, and label-free characteristics.

In the past ten years, the paper-based biosenors has attracted a lot of attention due to their large-scale production, low cost, versatility and ease of handling. Futhermore, recent research showed that the paper-based biosenor could detect the concentration of Phe in blood. However, the blood test is invasive, and draw blood for infants is difficult. Compared with the blood test, a urine test is noninvasive and likely to lead to higher patient compliance.

The objective of this study was the development of a novel paper-based biosensor based on PAL hybrid nanoflowers for urinary Phe measurement. For the construction of the paper-based biosensor, PAL-$Ca_3(PO_4)_2$ hybrid nanoflowers (PAL@NF) were firstly prepared by using crude PAL from recombinant BL21(DE3) *E. coli*. The catalytic activity and stability of the PAL@NF were investigated. Then, the PAL@NF was adsorbed on the surface of filter paper to obtain the paper-based biosensor. PAL in the PAL@NF can catalyze Phe in urine to produce a quantitative amount of t-CA which can be oxidized by the addition of a small amount of potassium permanganate, causing the fade of potassium permanganate. The dynamic range of the paper-based biosensor is 60 μM–2400 μM, and limit of detection is 60 μM. Furthermore, the test time was only about 10 min. Therefore, the paper-based biosensor is expected to become a home-test monitoring for PKU.

Acknowledgments

This work is partially supported by the Science and Technology Program of Tianjin, China (project no. 20ZYJDJC00080) and the Key Projects of Tianjin Natural Science Foundation, China (project no. 19JCZDJC38100).

References

[1] N. Blau, F.J. van Spronsen, H.L. Levy, Phenylketonuria, Lancet 376 (2010) 1417–1427.
[2] H.L. Levy, C.N. Sarkissian, C.R. Scriver, Phenylalanine ammonia lyase (PAL): from discovery to enzyme substitution therapy for phenylketonuria, Mol. Genet. Metab. 124 (2018) 223–229.
[3] W.B. Hanley, H. Demshar, M.A. Preston, A. Borczyk, W.E. Schoonheyt, J.T. Clarke, A. Feigenbaum, Newborn phenylketonuria (PKU) Guthrie (BIA) screening and early hospital discharge, Early Hum. Dev. 47 (1997) 87–96.
[4] V. Pierrat, N. Goubet, K. Peifer, J. Sizun, How can we evaluate developmental care practices prior to their implementation in a neonatal intensive care unit, Early Hum. Dev. 83 (2007) 415–418.
[5] B. Westrup, Newborn individualized developmental care and assessment program (NIDCAP) — family-centered developmentally supportive care, Early Hum. Dev. 83 (2007) 443–449.
[6] R.D. Christensen, E. Henry, S.E. Wiedmeier, J. Burnett, D.K. Lambert, Identifying patients, on the first day of life, at high-risk of developing parenteral nutrition-associated liver disease, J. Perinatol. 27 (2007) 284–290.
[7] N. Blau, J.B. Hennermann, U. Langenbeck, U. Lichter-Konecki, Diagnosis, classification, and genetics of phenylketonuria and tetrahydrobiopterin (BH4) deficiencies, Mol. Genet. Metab. 104 (2011) 2–9.
[8] P. Strisciuglio, D. Concolino, New strategies for the treatment of phenylketonuria (PKU), Metabolites 4 (2014) 1007–1017.
[9] S.M. Bell, D.J. Wendt, Y. Zhang, T.W. Taylor, S. Long, L. Tsuruda, B. Zhao, P. Laipis, P.A. Fitzpatrick, Formulation and PEGylation optimization of the therapeutic PEGylated phenylalanine ammonia lyase for the treatment of phenylketonuria, PLoS One 12 (2017), e0173269, .
[10] Z. Wang, Y.Z. Chen, S. Zhang, Z. Zhou, Investigation of a phenylalanine-biosensor system for phenylketonuria detection, Conf Proc IEEE Eng Med Biol Soc 2005 (2005) 1913–1916.
[11] J. Ge, J. Lei, R.N. Zare, Protein-inorganic hybrid nanoflowers, Nat. Nanotechnol. 7 (2012) 428–432.
[12] C. Altinkaynak, S. Tavlasoglu, N. Ozdemir, I. Ocsoy, A new generation approach in enzyme immobilization: organic-inorganic hybrid nanoflowers with enhanced catalytic activity and stability, Enzym. Microb. Technol. 93 (2016) 105–112.
[13] K.S. Park, B.S. Batule, M. Chung, K.S. Kang, T.J. Park, M.I. Kim, H.G. Park, A simple and eco-friendly one-pot synthesis of nuclease-resistant DNA–inorganic hybrid nanoflowers, J. Mater. Chem. B 5 (2017) 2231–2234.
[14] H.R. Luckarift, J.C. Spain, R.R. Naik, M.O. Stone, Enzyme immobilization in a biomimetic silica support, Nat. Biotechnol. 22 (2004) 211–213.
[15] C. Mateo, V. Grazu, J.M. Palomo, F. Lopez-Gallego, R. Fernandez-Lafuente, J.M. Guisan, Immobilization of enzymes on heterofunctional epoxy supports, Nat. Protoc. 2 (2007) 1022–1033.
[16] J. Kim, J.W. Grate, P. Wang, Nanobiocatalysis and its potential applications, Trends Biotechnol. 26 (2008) 639–646.
[17] J. Ge, D. Lu, Z. Liu, Z. Liu, Recent advances in nanostructured biocatalysts, Biochem. Eng. J. 44 (2009) 53–59.
[18] S. Ding, A.A. Cargill, I.L. Medintz, J.C. Claussen, Increasing the activity of immobilized enzymes with nanoparticle conjugation, Curr. Opin. Biotechnol. 34 (2015) 242–250.
[19] L. Zhu, L. Gong, Y.F. Zhang, R. Wang, J. Ge, Z. Liu, R.N. Zare, Rapid detection of phenol using a membrane containing laccase nanoflowers, 8 (2013) 2358–2360.
[20] I. Ocsoy, E. Dogru, S. Usta, A new generation of flowerlike horseradish peroxides as a nanobiocatalyst for superior enzymatic activity, Enzym. Microb. Technol. 75 (2015) 25–29.
[21] C. Altinkaynak, S. Tavlasoglu, R. Kalin, N. Sadeghian, H. Ozdemir, I. Ocsoy, N. Ozdemir, A hierarchical assembly of flower-like hybrid Turkish black radish peroxidase-Cu $^{2+}$ nanobiocatalyst and its effective use in dye decolorization, Chemosphere 182 (2017) 122–128.
[22] C. Altinkaynak, I. Yilmaz, Z. Koksal, H. Ozdemir, I. Ocsoy, N. Ozdemir, Preparation of lactoperoxidase incorporated hybrid nanoflower and its excellent activity and stability, Int. J. Biol. Macromol. 84 (2016) 402–409.
[23] I. Lee, H.J. Cheon, M.D. Adhikari, T.D. Tran, K.M. Yeon, M.I. Kim, J. Kim, Glucose oxidase-copper hybrid nanoflowers embedded with magnetic nanoparticles as an effective antibacterial agent, ational Journal of Biological Macromolecules 155 (2020) 1520–1531.
[24] Z. Wu, X. Li, F. Li, H. Yue, C. He, F. Xie, Z. Wang, Enantioselective transesterification of (R,S)-2-pentanol catalyzed by a new flower-like nanobioreactor, RSC Adv. 4 (2014) 33998–34002.
[25] H.R. Lee, M. Chung, M.I. Kim, S.H. Ha, Preparation of glutaraldehyde-treated lipase-inorganic hybrid nanoflowers and their catalytic performance as immobilized enzymes, Enzym. Microb. Technol. 105 (2017) 24–29.
[26] L.B. Wang, Y.C. Wang, R. He, A. Zhuang, X. Wang, J. Zeng, J.G. Hou, A new nanobiocatalytic system based on allosteric effect with dramatically enhanced enzymatic performance, J. Am. Chem. Soc. 135 (2013) 1272–1275.
[27] G. Zhu, R. Hu, Z. Zhao, Z. Chen, X. Zhang, W. Tan, Noncanonical self-assembly of multifunctional DNA nanoflowers for biomedical applications, J. Am. Chem. Soc. 135 (2013) 16438–16445.
[28] R. Hu, X. Zhang, Z. Zhao, G. Zhu, T. Chen, T. Fu, W. Tan, DNA nanoflowers for multiplexed cellular imaging and traceable targeted drug delivery, Angew. Chem. Int. Edit. 53 (2014) 5821–5826.
[29] L. Mei, G. Zhu, L. Qiu, C. Wu, H. Chen, H. Liang, S. Cansiz, Y. Lv, X. Zhang, W. Tan, Self-assembled multifunctional DNA nanoflowers for the circumvention of multidrug resistance in targeted anticancer drug delivery, Nano Res. 8 (2015) 3447–3460.
[30] A. Baldemir, N.B. Köse, N. Ildız, S. İlgün, S. Yusufbeyoğlu, V. Yilmaz, I. Ocsoy, Synthesis and characterization of green tea (*Camellia sinensis (L.) Kuntze*) extract and its major components-based nanoflowers: a new strategy to enhance antimicrobial activity, RSC Adv. 7 (2017) 44303–44308.
[31] Z. Zhang, Y. Zhang, R. Song, M. Wang, F. Yan, L. He, X. Feng, S. Fang, J. Zhao, H. Zhang, Manganese(II) phosphate nanoflowers as electrochemical biosensors for the high-sensitivity detection of ractopamine, Sensors Actuat B: Chem 211 (2015) 310–317.
[32] X. He, L. Chen, Q. He, H. Xiao, X. Zhou, H. Ji, Cytochrome P450 enzyme-copper phosphate hybrid nano-flowers with superior catalytic performances for selective oxidation of sulfides, Chin. J. Chem. 35 (2017) 693–698.
[33] X. Wang, J. Shi, Z. Li, S. Zhang, H. Wu, Z. Jiang, C. Yang, C. Tian, Facile one-pot preparation of chitosan/calcium pyrophosphate hybrid microflowers, ACS Appl. Mater. Interfaces 6 (2014) 14522–14532.
[34] L. Duan, H. Wang, J. Hou, Y. Zhang, V. Chen, A facile, bio-inspired synthetic route toward flower-like copper phosphate crystals with high specific surface area, Mater. Lett. 161 (2015) 601–604.
[35] Y. Liu, J. Chen, M. Du, X. Wang, X. Ji, Z. He, The preparation of dual-functional hybrid nanoflower and its application in the ultrasensitive detection of disease-related biomarker, Biosens. Bioelectron. 92 (2017) 68–73.
[36] M. Zhang, R. Peltier, M. Zhang, H. Lu, H. Bian, Y. Li, Z. Xu, Y. Shen, H. Sun, Z. Wang, In situ reduction of silver nanoparticles on hybrid polydopamine–copper phosphate nanoflowers with enhanced antimicrobial activity, J. Mater. Chem. B 5 (2017) 5311–5317.
[37] N. ILdiz, A. Baldemir, C. Altinkaynak, N. Ozdemir, V. Yilmaz, I. Ocsoy, Self assembled snowball-like hybrid nanostructures comprising *Viburnum opulus L.* extract and metal ions for antimicrobial and catalytic applications, Enzym. Microb. Technol. 102 (2017) 60–66.
[38] C. Celik, N. ILdiz, I. Ocsoy, Building block and rapid synthesis of catecholamines-inorganic nanoflowers with their peroxidase-mimicking and antimicrobial activities, Sci. Rep. 10 (2020) 2903.
[39] F.D. Koca, D.D. Yilmaz, N.E. Onmaz, E. Yilmaz, I. Ocsoy, Green synthesis of allicin based hybrid nanoflowers with evaluation of their catalytic and antimicrobial activities, Biotechnol. Lett. 42 (2020) 1683–1690.
[40] C. Celik, D. Tasdemir, A. Demirbas, A. Kati, O.T. Gul, B. Cimen, I. Ocsoy, Formation of functional nanobiocatalysts with a novel and encouraging immobilization approach and their versatile bioanalytical applications, RSC Adv. 8 (2018) 25298–25303.
[41] B.S. Batule, K.S. Park, S. Gautam, H.J. Cheon, M.I. Kim, H.G. Park, Intrinsic peroxidase-like activity of sonochemically synthesized protein copper nanoflowers and its application for the sensitive detection of glucose, Sensors Actuators B Chem. 283 (2019) 749–754.
[42] Y.X. Li, G.M. Xie, J.H. Qiu, D.D. Zhou, D. Gou, Y.Y. Tao, Y. Li, H. Chen, A new biosensor based on the recognition of phages and the signal amplification of organic-inorganic hybrid nanoflowers for discriminating and quantitating live pathogenic bacteria in urine, Sensors Actuat B: Chem 258 (2018) 803–812.
[43] L. Zhu, L. Gong, Y.F. Zhang, R. Wang, J. Ge, Z. Liu, R.N. Zare, Rapid detection of phenol using a membrane containing laccase nanoflowers, Chem. Asian J. 8 (2013) 2358–2360.
[44] H.J. Cheon, M.D. Adhikari, M. Chung, T.D. Tran, J. Kim, M.I. Kim, Magnetic nanoparticles-embedded enzyme-inorganic hybrid nanoflowers with enhanced peroxidase-like activity and substrate channeling for glucose biosensing, Advanced Healthcare Materials 8 (2019) 1801507.
[45] M. Chung, T.L. Nguyen, T.O.N. Tran, H.H. Yoon, I.T. Kim, M.I. Kim, Ultrarapid sonochemical synthesis of enzyme-incorporated copper nanoflowers and their application to mediatorless glucose biofuel cell, Applied Surface Sciences 429 (2018) 203–209.
[46] G. Thiessen, R. Robinson, K. De Los Reyes, R.J. Monnat Jr., E. Fu, Conversion of a laboratory-based test for phenylalanine detection to a simple paper-based format and implications for PKU screening in low-resource settings, Analyst 140 (2015) 609–615.
[47] R. Ye, C. Zhu, Y. Song, Q. Lu, X. Ge, X. Yang, M.J. Zhu, D. Du, H. Li, Y. Lin, Bioinspired synthesis of all-in-one organic-inorganic hybrid nanoflowers combined with a handheld pH meter for on-site detection of food pathogen, Small 12 (2016) 3094–3100.
[48] R. Ye, C. Zhu, Y. Song, J. Song, S. Fu, Q. Lu, X. Yang, M.J. Zhu, D. Du, H. Li, Y. Lin, One-pot bioinspired synthesis of all-inclusive protein-protein nanoflowers for point-of-care bioassay: detection of E. coli O157:H7 from milk, Nanoscale 8 (2016) 18980–18986.
[49] C.M. Moreira, S.V. Pereira, J. Raba, F.A. Bertolino, G.A. Messina, Paper-based enzymatic platform coupled to screen printed graphene-modified electrode for the fast neonatal screening of phenylketonuria, Clin. Chim. Acta 486 (2018) 59–65.
[50] B. Zhang, P. Li, H. Zhang, H. Wang, X. Li, L. Tian, N. Ali, Z. Ali, Q. Zhang, Preparation of lipase/Zn3(PO4)2 hybrid nanoflower and its catalytic performance as an immobilized enzyme, Chem. Eng. J. 291 (2016) 287–297.
[51] S.K.S. Patel, H. Choi, J.-K. Lee, Multimetal-based inorganic–protein hybrid system for enzyme immobilization, ACS Sustain. Chem. Eng. 7 (2019) 13633–13638.
[52] R.M. Shah, P. D'Mello A, Strategies to maximize the encapsulation efficiency of phenylalanine ammonia lyase in microcapsules, Int. J. Pharm. 356 (2008) 61–68.
[53] J. Cui, Y. Zhao, Z. Tan, C. Zhong, P. Han, S. Jia, Mesoporous phenylalanine ammonia lyase microspheres with improved stability through calcium carbonate templating, Int. J. Biol. Macromol. 98 (2017) 887–896.
[54] M. Deon, A. Sitta, J.L. Faverzani, G.B. Guerreiro, B. Donida, D.P. Marchetti, C.P. Mescka, G.S. Ribas, A.S. Coitinho, M. Wajner, C.R. Vargas, Urinary biomarkers of oxidative stress and plasmatic inflammatory profile in phenylketonuric treated patients, Int. J. Dev. Neurosci. 47 (2015) 259–265.